

Lattice QCD Determination of g_A

André Walker-Loud*, Lawrence Berkeley National Laboratory

Evan Berkowitz, University of Maryland

David A. Brantley, Arjun Gambhir, Pavlos Vranas, Lawrence Livermore National Laboratory

Chris Bouchard, University of Glasgow

Chia Cheng Chang, RIKEN-iTHEMS

M.A. Clark, NVIDIA Corporation

Nicolas Garron, Liverpool Hope University

Bálint Joó, Thomas Jefferson National Accelerator Facility

Thorsten Kurth NERSC, Lawrence Berkeley National Laboratory

Henry Monge-Camacho, Amy Nicholson, University of North Carolina Chapel Hill

Christopher J Monahan, Kostas Orginos, The College of William & Mary

Enrico Rinaldi, Arithmer Inc. & RIKEN-iTHEMS

The nucleon axial coupling, g_A , is a fundamental property of protons and neutrons, dictating the strength with which the weak axial current of the Standard Model couples to nucleons, and hence, the lifetime of a free neutron. The prominence of g_A in nuclear physics has made it a benchmark quantity with which to calibrate lattice QCD calculations of nucleon structure and more complex calculations of electroweak matrix elements in one and few nucleon systems. There were a number of significant challenges in determining g_A , notably the notorious exponentially-bad signal-to-noise problem and the requirement for hundreds of thousands of stochastic samples, that rendered this goal more difficult to obtain than originally thought.

I will describe the use of an unconventional computation method, coupled with “ludicrously” fast GPU code, access to publicly available lattice QCD configurations from MILC and access to leadership computing that have allowed these challenges to be overcome resulting in a determination of g_A with 1% precision and all sources of systematic uncertainty controlled. I will discuss the implications of these results for the convergence of $SU(2)$ Chiral Perturbation theory for nucleons, as well as prospects for further improvements to g_A (sub-percent precision, for which we have preliminary results) which is part of a more comprehensive application of lattice QCD to nuclear physics. This is particularly exciting in light of the new CORAL supercomputers coming online, Sierra and Summit, for which our lattice QCD codes achieve a machine-to-machine speed up over Titan of an order of magnitude.

The 9th International workshop on Chiral Dynamics
17-21 September 2018
Durham, NC, USA

*Speaker.

1. Motivation

The nucleon axial coupling, g_A , often called the nucleon axial charge, is a ubiquitous quantity in nuclear physics. The strength of this coupling controls the rate of nuclear reactions, beta-decay, and the pion-exchange contributions to the nucleon-nucleon potential. Furthermore, it governs the lifetime of the free neutron and strongly influences the primordial abundances of H and ^4He .

While the nucleon axial coupling has been measured extremely precisely experimentally, yielding a global average value of $g_A = 1.2732(23)$ [1] (and updated results that are substantially more precise [2]), first-principles calculations of this quantity provide a stringent test of the limits of the Standard Model (SM) and could potentially point to new physics. For example, the so-called “neutron lifetime puzzle” (for a discussion, see Ref [3]), a 4-sigma discrepancy between experimental measurements utilizing beams of neutrons versus those using trapped ultracold neutrons, could point to new beyond the SM decay modes. A theoretical calculation rooted in the SM may help to clarify this puzzle. Furthermore, because it is so well-measured and ubiquitous, g_A provides an important benchmark for lattice QCD (LQCD) calculations related to nuclear physics. Systematic errors of this quantity must be fully understood and controlled before calculations of more challenging, and less experimentally well-known, quantities, such as the axial form factor of the nucleon, can be regarded as reliable.

In these proceedings I will discuss the advances made that have enabled a recent calculation of g_A to 1% precision, with all systematics controlled. I will also discuss the implications of the results for the use of $SU(2)$ Chiral Perturbation theory for nucleons. Finally, I will present a preliminary sub-precision update of our results with improved statistics at the physical pion mass achieved using early science time on Sierra at LLNL, and discuss future prospects for further reduction of uncertainties. This is an exciting time as we move towards the exascale era in which we aim to build a quantitative bridge between QCD and theories of nuclear physics, with the aim of building a predictive theory of nuclear structure and reactions, rooted in the Standard Model [4], beginning with properties of the nucleon, moving to light nuclei (see CD2018 talk of Z. Davoudi) and coupling to theories of many body nuclear physics (see the CD2018 talks of M. Piarulli and S. Pastore).

2. A percent-level determination of g_A from QCD

We have recently determined g_A with an unprecedented percent-level of uncertainty [5]

$$g_A = 1.2711(103)^s(39)^\chi(15)^a(04)^V(55)^M. \quad (2.1)$$

The sources of uncertainty are statistical (s), extrapolation to the physical pion mass (χ), continuum extrapolation (a), infinite volume extrapolation (V) and a model average uncertainty (M). Prior to this result, it was estimated that a 2% uncertainty could be achieved with near-exascale computing (such as Summit at OLCF) by 2020 [6]. There were several key features of our calculation that enabled a determination with 1% uncertainty with the previous generation of supercomputers:

1. The use of an unconventional strategy motivated by the Feynman-Hellmann Theorem (FHT) [7];
2. Access to publicly available configurations that enabled the full physical point extrapolation, in this case the $N_f = 2 + 1 + 1$ HISQ [8] configurations generated by MILC [9];

3. *Ludicrously* fast GPU code for lattice QCD, in this case the QUDA library [10, 11];
4. Access to leadership class computing at LLNL through the Grand Challenge Program and Titan at OLCF through the DOE INCITE program.

I will describe the unconventional method in Sec. 2.1 and describe the comprehensive analysis that leads to the quoted uncertainty breakdown in Sec. 2.2, including the stability of the final extrapolation. Implications for $SU(2)$ baryon χ PT will be discussed in Sec. 2.3 followed by a discussion of expected improvements in precision with some preliminary results in Sec. 3.

2.1 An unconventional method

The two most pressing challenges in applying LQCD to nucleon elastic structure calculations are the exponentially bad signal-to-noise (S/N) problem [12] and contamination from excited states. To overcome these challenges, we “invented” a new method for performing the calculations [7] (after “inventing” this method, of course we realized it has been around since the 80’s [13, 14] and there are more recent applications that are very similar [15, 16, 17, 18, 19]).

This unconventional method can be derived by applying the FHT to the effective mass of a correlation function in the presence of a background field. Consider a two-point correlation function coupled to a external current

$$\begin{aligned} C_\lambda(t) &= \langle \Omega | \phi(t) \phi^\dagger(0) | \Omega \rangle_\lambda \\ &= \frac{1}{Z_\lambda} \int D[\phi] e^{-S} e^{-\lambda \int d^4x j_\lambda(x)} \phi(t) \phi^\dagger(0), \quad \text{with} \quad Z_\lambda = \int D[\phi] e^{-S} e^{-\lambda \int d^4x j_\lambda(x)} \\ &= \sum_n |\langle n | \phi^\dagger | \Omega \rangle_\lambda|^2 e^{-E_n^\lambda t} \end{aligned} \quad (2.2)$$

The effective mass of this system will asymptote to the ground state energy for large t

$$m_\lambda^{\text{eff}}(t, \tau) = \frac{1}{\tau} \ln \left(\frac{C_\lambda(t)}{C_\lambda(t + \tau)} \right) \xrightarrow{t \rightarrow \infty} E_0^\lambda. \quad (2.3)$$

The Feynman-Hellmann Theorem in quantum mechanics relates matrix elements to shifts in the spectrum, $\partial_\lambda E_n^\lambda|_{\lambda=0} = \langle n | H_\lambda | n \rangle$. If we “follow our nose” and apply the FHT to the effective mass, we derive a new correlation function that can be used to compute matrix elements in QFT [7]

$$\begin{aligned} \left. \frac{\partial m_\lambda^{\text{eff}}(t, \tau)}{\partial \lambda} \right|_{\lambda=0} &= \frac{1}{\tau} \left[\frac{-\partial_\lambda C_\lambda(t + \tau)}{C(t + \tau)} - \frac{-\partial_\lambda C_\lambda(t)}{C(t)} \right]_{\lambda=0} \\ &= g_\lambda + z_{10} \left(\frac{e^{-(t+\tau)\Delta_{10}} - e^{-t\Delta_{10}}}{\tau} \right) + \dots, \end{aligned} \quad (2.4)$$

where g_λ is the matrix element of the ground state with the current, $g_\lambda = (2E_0)^{-1} \langle 0 | j_\lambda | 0 \rangle$,

$$-\partial_\lambda C_\lambda(t) \Big|_{\lambda=0} = \frac{\partial_\lambda Z_\lambda}{Z} \Big|_{\lambda=0} C(t) + \frac{1}{Z} \int D[\phi] e^{-S} \int d^3x_\lambda dt_\lambda O(t) j_\lambda(t_\lambda, x_\lambda) O^\dagger(0), \quad (2.5)$$

is a new correlation function we can compute in the $\lambda = 0$ vacuum, $C(t) = C_\lambda(t)|_{\lambda=0}$, $\Delta_{10} = E_1 - E_0$, z_{10} is related to the ratio of the overlap of the interpolating operator onto the first excited state versus the ground state and the \dots represent contributions from higher excited states (see Ref. [7] for a complete expression). There are a few key features of this expression, Eq. (2.4):

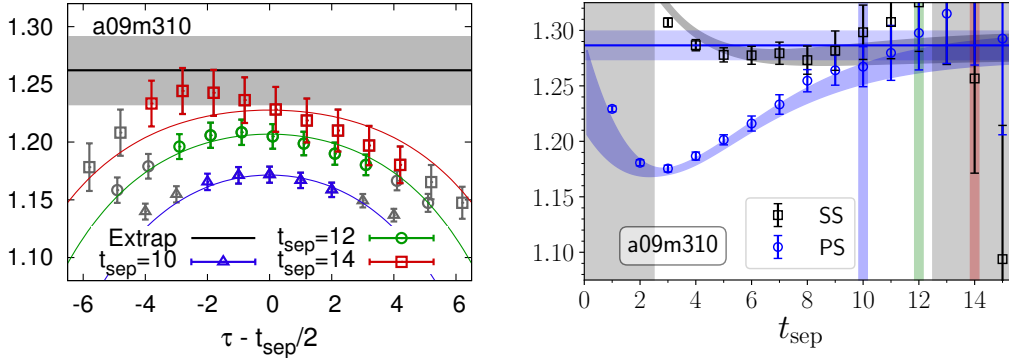


Figure 1: Left: Standard three-point function calculation from Ref. [20]. Right: Sample fit from Ref. [5] on the same $a \sim 0.09$ fm, $m_\pi \sim 310$ MeV (a09m310) HISQ ensemble. The vertical gray bands indicate results excluded from the fit. The two sets of data correspond to two different sink smearings with a point (P) and smeared (S) sink and both use a smeared source. The curves result from a simultaneous two-state fit to six correlation functions (SS and PS for the two-point, g_V and g_A correlation functions) while the horizontal band is the ground state matrix element. The vertical bands correspond to the three values of t_{sep} used in Ref. [20], $t_{\text{sep}} = 10$ (blue), 12 (green), and 14 (red). The y-axis in both figures are the same. As is evident, the FH method [7] enables the use of many more values of t_{sep} as well as earlier values that are stochastically more precise and less prone to stochastic fluctuations, allowing for a more stable and precise extrapolation to $t_{\text{sep}} \rightarrow \infty$.

1. The excited state contributions are not only suppressed exponentially by the mass gap Δ_{10} , but they are further suppressed by the difference between neighboring times separated by τ (the user is free to choose τ and we typically chose $\tau = 1$). This enables a fit to the correlation function to begin earlier in Euclidean time than is generally possible for three-point correlation functions, where the stochastic signal is exponentially more precise;
2. Three point correlation functions depend upon two time variables, the source/sink separation time, t (often denoted t_{sep}) and the current insertion time, t_λ . Eq. (2.4) only depends upon the source/sink separation time, simplifying the analysis;
3. In standard three point function calculations, $t = t_{\text{sep}}$ is fixed and so multiple calculations must be performed to extrapolate to large t . In the implementation of Eq. (2.4), all values of t are accessible with a single calculation, although for fixed current and momentum transfer;
4. Unlike other methods [17, 18, 19], the variation of background field effects are not numerically implemented, but rather, the strength of the coupling to the background field, λ is used to analytically track the dependence and derive this additional correlation function, Eq. (2.5) which is evaluated at $\lambda = 0$. Note, in the difference in Eq. (2.4), the dependence upon the vacuum matrix element, the first term in Eq. (2.5), exactly cancels.

It is useful to compare and contrast results from the two methods, which we do in Figure 1. A more exhaustive study of the sensitivity of the ground state matrix elements with respect to choices of $t_{\text{min,max}}$ on all correlation functions and all ensembles was performed and reported in Ref. [5]. The final fits are very sensitive to the initial guess of all the fit parameters. We therefore used a Bayesian fit to precondition the initial guess of a final two-state frequentist minimization, resulting in stable frequentist fits. The bootstrap distributions of the ground state values are all close to Gaussian distributed with minimal tails, a further indication of the stability of the correlator fits.

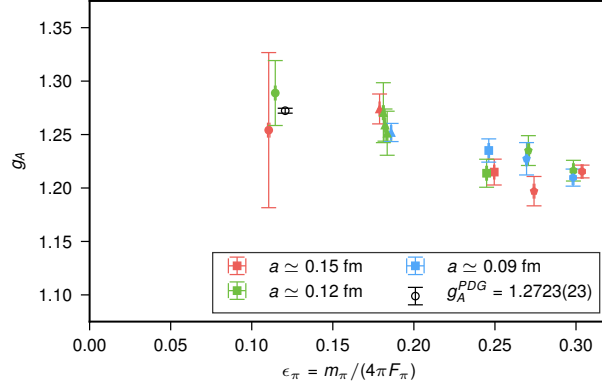


Figure 2: Renormalized values of g_A from Ref. [5]. The results show a very mild dependence upon both ϵ_π and $\epsilon_a^2 = a^2/(4\pi w_0^2)$, indicating a mild extrapolation. While the results at the physical pion mass are significantly less precise than at heavier pion masses, the value on the a12m130 (green) ensemble has a 2.3% uncertainty, which was the most precise value at the physical pion mass at the time of publication [5].

2.2 Extrapolation to the physical point

In order to control the extrapolation to the physical point, several values of the lattice spacing, light quark masses and volumes must be used. The only set of configurations that are publicly available with sufficient variation in these parameters are the $N_f = 2 + 1 + 1$ HISQ [8] ensembles generated by the MILC Collaboration [9] which have been generated with six lattice spacings now spanning $0.03 \lesssim a \lesssim 0.15$ fm [21] and three pion masses $m_\pi \sim \{130, 220, 310\}$ MeV. In a previous study, we found that these three pion masses were not sufficient to eliminate the model dependence in the chiral extrapolation to the physical pion mass [22]. Therefore, we generated six new ensembles with $a \sim \{0.09, 0.12, 0.15\}$ fm at $m_\pi \sim \{350, 400\}$ MeV. In total, we performed the calculation on 16 ensembles with $0.09 \lesssim a \lesssim 0.15$ fm, $130 \lesssim m_\pi \lesssim 400$ MeV and a dedicated volume study with three volumes on the a12m220 ensemble (we use the very convenient and descriptive shorthand notation for ensembles [23]).

To perform the calculation, we first used gradient-flow [24, 25, 26] to smooth the UV fluctuations with a flow-time of $t_{gf} = 1.0$ in lattice units. We then solved Möbius Domain-Wall Fermions (MDWF) [27] in the valence sector for an MDWF on gradient-flowed HISQ action [28]. By holding the flow-time fixed in lattice units, any flow-time dependence should vanish as the continuum limit is taken. With $t_{gf} = 1$, we found that $m_{\text{res}} \lesssim 0.1 \times m_l$ for all ensembles with reasonable values of L_5 , minimizing the residual chiral symmetry breaking. Further, because of the near chiral symmetry of the action, we found that the non-perturbative value of $Z_A = Z_V$ to one part in 10^4 , greatly simplifying the renormalization of the matrix elements; the physical value of g_A on each ensemble is simply given by \hat{g}_A/\hat{g}_V where $\hat{g}_{A,V}$ are the bare values of the charges, as $Z_V \hat{g}_V = 1$ by definition. Our renormalized values of g_A are shown in Figure 2.

g_A is a dimensionless quantity and so it is useful to construct dimensionless parameters that can be used to perform the three extrapolations to the physical point. In order to perform the chiral extrapolation, we use the small parameter

$$\epsilon_\pi = \frac{m_\pi}{4\pi F_\pi}, \quad (2.6)$$

where $F_\pi \simeq 92$ MeV at the physical point. This is also convenient as ε_π is the small parameter which controls the chiral expansion in heavy-baryon χ PT [29]. At fixed m_π , the finite volume corrections scale asymptotically in the volume as $e^{-m_\pi L}$ [30] where L is the size of the spatial box, for $m_\pi L \gtrsim 4$. The leading finite volume corrections to g_A were determined in Ref. [31].

To parameterize the continuum extrapolation, we introduce the small parameter

$$\varepsilon_a^2 = \frac{1}{4\pi} \frac{a^2}{w_0^2}, \quad (2.7)$$

where w_0 is a gradient-flow scale [32] which is $w_0 \sim 0.17$ fm. For our MDWF on HISQ action, the leading discretization effects scale as ε_a^2 which follows from the Symanzik expansion of the lattice action [33, 34] near the continuum limit.

At next-to-next-to-leading order (NNLO) in the chiral expansion, g_A is given by [35]

$$g_A = g_0 - \varepsilon_\pi^2 [(g_0 + 2g_0^3) \ln(\varepsilon_\pi^2) - c_2] + g_0 c_3 \varepsilon_\pi^3, \quad (2.8)$$

where g_0 , c_2 and c_3 are low-energy-constants (LECs) that must be determined from analyzing LQCD results and/or experimentally measured observables. The NLO expression (up to $O(\varepsilon_\pi^2)$) was insufficient to describe the results for $m_\pi \lesssim 310$ MeV and the NNLO expression has three LECs, so at least four values of the pion mass are required to fit the pion mass dependent LECs.

Given the very mild pion mass dependence observed in the results and the observed challenges with the convergence of baryon χ PT [36, 37, 38] we also explore a simple Taylor expansion both as an expansion about ε_π^2 and ε_π . In each case, we explore the convergence of the expansions by performing each extrapolation with two different truncation orders. For χ PT, as the NNLO fit is the first to have a reasonable quality of fit, we add the counterterm from N³LO to explore the convergence. An honest full N³LO fit is not possible as that contains 5 LECs and our results have 5 pion mass values (see Sec. 2.3). For the Taylor expansion fits, we perform both an NLO and NNLO fit where in each case, LO is just a constant in ε_π . χ PT fits with explicit delta-resonance degrees of freedom were not included as our numerical results do not include the $N \rightarrow \Delta$ and $\Delta \rightarrow \Delta$ matrix elements needed to constrain these contributions to g_A and so too much prior knowledge from phenomenology would be required to stabilize the analysis with these states. It should be noted that the large- N_c expansion leads to a cancellation between virtual nucleon and delta contributions which can help explain the mild pion mass dependence [39, 40].

The extrapolation analysis is performed in a Bayesian Framework allowing for a weighted model average to be performed. By performing this semi-exhaustive chiral extrapolation analysis, we hope to remove theorist bias in the ‘‘correct’’ extrapolation form and let the numerical results dictate the preferred extrapolation. Such a user unbiased approach is simple in this case in which the results have very mild pion mass dependence, but would be more challenging for quantities, such as the proton charge radius, which has a $\ln(m_\pi)$ divergence. The resulting analysis is given in Table 1. As can be seen, the Taylor expansion fits are strongly favored over the χ PT fits. In part, this is due to the strong cancellation among different orders in the χ PT function that must occur to produce such a mild pion mass dependence.

It is also important to check for the sensitivity of the final result upon the heavy pion mass points as these are the most statistically precise, but expected to have the largest systematic correction from the chiral extrapolation. Such a study can be achieved either by adding more terms to

Table 1: Six chiral extrapolation models are considered. For each fit, the *augmented* χ^2/dof , the *log Gaussian Bayes Factor* ($\log\text{GBF}$) $\mathcal{L}(D|M_k)$, the normalized weight of the fit determined from $\exp(\log\text{GBF}) P(M_k|D)$ and the resulting posterior at the physical point $P(g_A|M_k)$ is given. The final uncertainty arises from the weighted average variance and the second is from the model variance, see Eq. (S26) of Ref. [5].

Fit	χ^2/dof	$\mathcal{L}(D M_k)$	$P(M_k D)$	$P(g_A M_k)$
NNLO χPT	0.727	22.734	0.033	1.273(19)
NNLO+ct χPT	0.726	22.729	0.033	1.273(19)
NLO Taylor ε_π^2	0.792	24.887	0.287	1.266(09)
NNLO Taylor ε_π^2	0.787	24.897	0.284	1.267(10)
NLO Taylor ε_π	0.700	24.855	0.191	1.276(10)
NNLO Taylor ε_π	0.674	24.848	0.172	1.280(14)
average				1.271(11)(06)

the chiral extrapolation functions or by studying the result as the heavy mass points are cut. The former method is already incorporated in our analysis in Table 1. The latter method can not easily be used to quantitatively compare/average fits as fits that use different data sets can not easily be compared to each other as the absolute normalization, or *evidence*, changes as data is added or removed. Nevertheless, it is instructive to see how much the final extrapolation changes as data far from the physical point is removed. We studied the sensitivity to data truncation by considering fits with $m_\pi \lesssim 350$ MeV and $m_\pi \lesssim 310$ MeV as well as all data ($m_\pi \lesssim 400$ MeV). Further, we studied the extrapolation when we cut the $a \sim 0.15$ fm or $a \sim 0.09$ fm ensembles. In addition to these data truncations, we studied the sensitivity to turning on/off the finite volume corrections, adding additional discretization corrections and increasing the size of the prior widths used to constrain the higher order corrections. Results from this analysis are shown in Figure 3. As can be seen, the final extrapolated answer is very stable under all such variations/data truncations.

2.3 Implications for $SU(2)$ baryon chiral perturbation theory

As this is the Chiral Dynamics Workshop, I will spend some time discussing the implications for $SU(2)$ baryon χPT from these results. The N^3LO extrapolation formula is known with the N^3LO terms given by (the \ln^2 coefficients differ from Ref. [41] as we have converted $F \rightarrow F_\pi$)

$$\delta g_A^{\text{N}^3\text{LO}} = \varepsilon_\pi^4 \left[c_4 + \tilde{\gamma}_4 \ln(\varepsilon_\pi^2) + \left(\frac{2}{3}g_0 + \frac{37}{12}g_0^3 + 4g_0^5 \right) \ln^2(\varepsilon_\pi^2) \right], \quad (2.9)$$

where c_4 and $\tilde{\gamma}_4$ are new LECs that must be constrained. While an honest fit with the full N^3LO formula can not be performed (there are 5 LECs parameterizing the pion mass dependence and 5 values of m_π in the numerical results), we can examine the stability of chiral extrapolation by performing this N^3LO analysis, which is shown in Figure 4. The right panels show the cumulative convergence of the fit. For the NNLO analysis, one observes a rapid drop of the LO+NLO (NLO) contributions as ε_π is increased slightly above its physical value. At the physical pion mass, the NNLO contributions are opposite in sign and about twice as large as the NLO contributions. Adding the N^3LO terms makes this situation worse: the NLO contribution dives faster and the

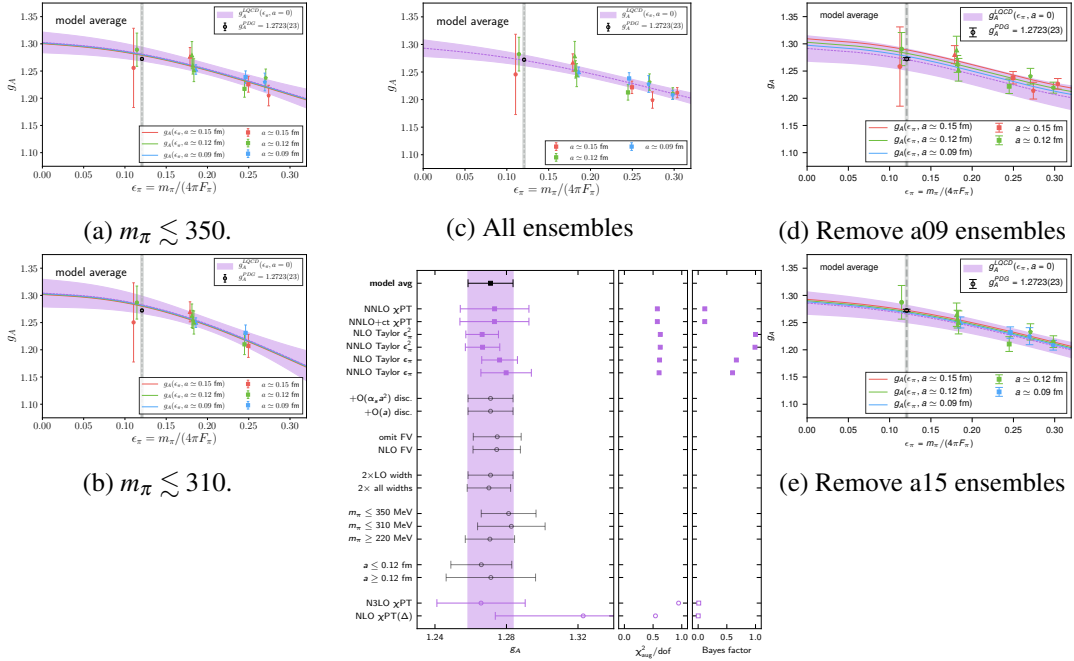


Figure 3: Stability of the extrapolation as prior widths are varied, data is truncated and various continuum extrapolation models are included. The magenta band in summary plot (bottom middle) is from the model average (top 6 entries) and displayed to guide the eye. For all changes, the final extrapolation lies within one standard deviation of the final answer, demonstrating the stability of the result.

convergence pattern worsens. At the physical pion mass, we find the order-by-order contributions

$N^m \text{LO}$	δg_A^{LO}	δg_A^{NLO}	$\delta g_A^{\text{N}^2 \text{LO}}$	$\delta g_A^{\text{N}^3 \text{LO}}$
$\text{N}^2 \text{LO}$	1.237(34)	-0.026(30)	0.062(14)	—
$\text{N}^3 \text{LO}$	1.296(76)	-0.19(12)	0.045(63)	0.117(66)

for which there are strong cancellations order-by-order for $SU(2)$ heavy-baryon χPT . It is not expected the covariant formulation of baryon χPT [42] will improve the situation but the inclusion of explicit delta-degrees of freedom should. However, in the case of the nucleon mass, the virtual delta-corrections add with the same sign and so they will make the convergence pattern of the nucleon mass worse. All in all, lattice results are indicating that $SU(2)$ heavy-baryon χPT without delta-degrees of freedom is a failing perturbative expansion, even at the physical pion mass.

3. Updates and Outlook

Improving the precision of g_A from QCD is interesting for several reasons. Already, the precision of g_A [5] sets the limiting constraint on right-handed BSM currents [43] and further improvements are welcome. A reduction of the uncertainty to 0.2% would place an uncertainty on the predicted neutron lifetime, using g_A from QCD, at a level sufficient to provide 4-sigma discriminating resolution. This is a tractable problem for LQCD in the exascale computing era. However, to reduce the uncertainty below 0.5% requires a comparison with the newly uncovered QED radiative corrections to β -decay [44] (there is also an improved determination of the inner radiative corrections [45, 46] which can be tested with LQCD as well [47]).

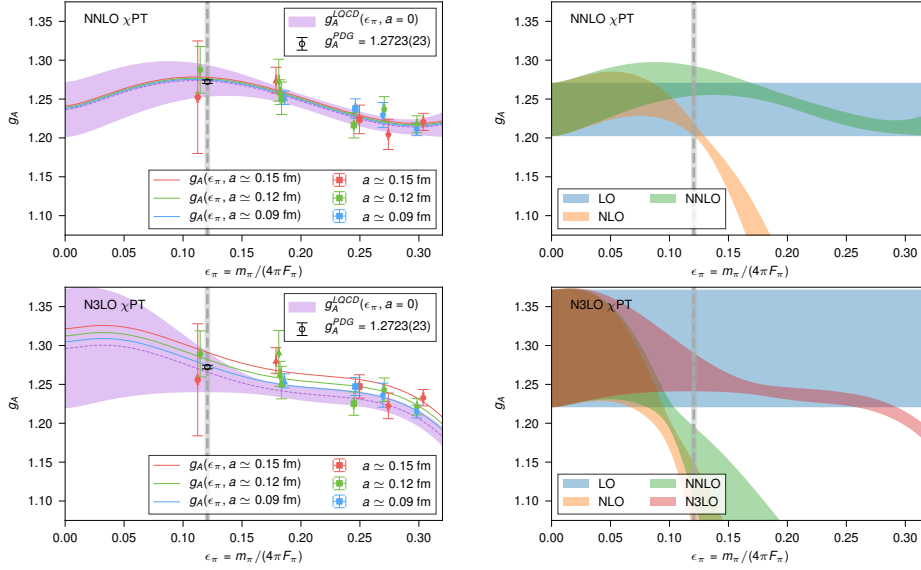


Figure 4: Left: the NNLO and $\mathcal{N}^3\text{LO}$ extrapolation fits plotted versus ϵ_π . Right: The cumulative contribution up to a given order versus ϵ_π .

In the current near-exascale era, we will see significant improvements. Machine-to-machine, for our LQCD applications, Summit is 15 times faster than Titan [48]. We are continuing to improve our determination of g_A as part of a more comprehensive program to determine the nucleon elastic form factors. We were early-science users on the Sierra Supercomputer at LLNL in late 2018. In Figure 5, we show our preliminary updated results with this early science time (right) with our published result [5] (left). Of note

1. The a12m130 ensemble (left most green point) is the most expensive one used in this work. In our published result, we had three sources per configuration, which cost more than all other ensembles combined. These were produced with our 2016 INCITE allocation on Titan. In 2.5 weekends on Sierra, we were able to produce 16 sources per configuration, and the updated result now has 32 sources, can be fit with an unconstrained 3-state frequentist fit, and the precision on this ensemble is sub-percent;
2. The a15m130 ensemble (left most red point) was too noisy for this project, likely from the small volume ($L = 32, T = 48$ with $m_\pi L \sim 3.23$). We generated a new ensemble, a15m135XL ($L = 48, T = 64$) with 4 streams of 250 configurations each. The right panel of Figure 5 has a result from this ensemble with 8 sources per configuration.
3. Our preliminary update with new a12m130 and a15m135XL results has a 0.74% uncertainty

$$g_A^{\text{QCD}} = 1.2711(125) \rightarrow 1.2642(93). \quad (3.1)$$

4. We have generated new ensembles at $m_\pi \sim \{180, 260\}$ MeV to increase the density of light pion mass results, and help explore the convergence of baryon χPT .
5. To achieve a 0.5% uncertainty, a fourth lattice spacing at $a \sim 0.06$ fm is likely required with our MDWF on gradient-flowed HISQ action [28].

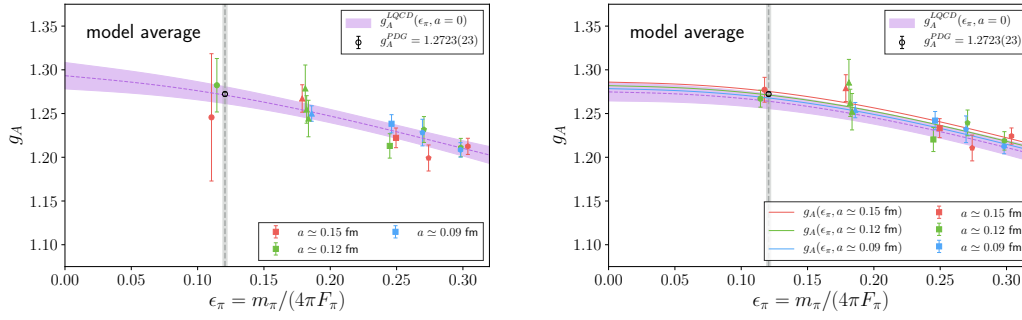


Figure 5: Left: our published model-average extrapolation [5]. Right: A preliminary update of our results with improved statistics at the physical pion mass enabled through early science time on Sierra at LLNL.

Acknowledgments We thank the LLNL Multiprogrammatic and Institutional Computing program for Grand Challenge allocations on the LLNL supercomputers, Surface, RZHasGPU and Vulcan. This research also used the NVIDIA GPU-accelerated Titan supercomputer at the Oak Ridge Leadership Computing Facility at the Oak Ridge National Laboratory, which is supported by the Office of Science of the U.S. Department of Energy under Contract No. DE-AC05-00OR22725, through an award of computer time provided by the INCITE program. This research also used the Sierra computer operated by the Lawrence Livermore National Laboratory for the Office of Advanced Simulation and Computing and Institutional Research and Development, NNSA Defense Programs within the U.S. Department of Energy, during the Early Science period.

References

- [1] PARTICLE DATA GROUP collaboration, M. Tanabashi et al., *Review of particle physics*, *Phys. Rev. D* **98** (2018) 030001.
- [2] B. MÅd'rkisch et al., *Measurement of the Weak Axial-Vector Coupling Constant in the Decay of Free Neutrons Using a Pulsed Cold Neutron Beam*, *Phys. Rev. Lett.* **122** (2019) 242501 [1812.04666].
- [3] A. Czarnecki, W. J. Marciano and A. Sirlin, *Neutron Lifetime and Axial Coupling Connection*, *Phys. Rev. Lett.* **120** (2018) 202002 [1802.01804].
- [4] C. Drischler, W. Haxton, K. McElvain, E. Mereghetti, A. Nicholson, P. Vranas et al., *Towards grounding nuclear physics in QCD*, 2019, 1910.07961.
- [5] C. C. Chang, A. Nicholson, E. Rinaldi, E. Berkowitz, N. Garron, D. A. Brantley et al., *A per-cent-level determination of the nucleon axial coupling from quantum chromodynamics*, *Nature* **558** (2018) 91 [1805.12130].
- [6] Science Talk 1: Cold Nuclear Physics, USQCD Annual Progress Review to the US DOE <http://www.usqcd.org/reviews/June2016Review/agenda.html>: Accessed 2018-05-31.
- [7] C. Bouchard, C. C. Chang, T. Kurth, K. Orginos and A. Walker-Loud, *On the Feynman-Hellmann Theorem in Quantum Field Theory and the Calculation of Matrix Elements*, *Phys. Rev.* **D96** (2017) 014504 [1612.06963].
- [8] HPQCD, UKQCD collaboration, E. Follana, Q. Mason, C. Davies, K. Hornbostel, G. P. Lepage, J. Shigemitsu et al., *Highly improved staggered quarks on the lattice, with applications to charm physics*, *Phys. Rev.* **D75** (2007) 054502 [hep-lat/0610092].

- [9] MILC collaboration, A. Bazavov et al., *Lattice QCD ensembles with four flavors of highly improved staggered quarks*, *Phys. Rev.* **D87** (2013) 054505 [[1212.4768](#)].
- [10] M. Clark, R. Babich, K. Barros, R. Brower and C. Rebbi, *Solving Lattice QCD systems of equations using mixed precision solvers on GPUs*, *Comput.Phys.Commun.* **181** (2010) 1517 [[0911.3191](#)].
- [11] R. Babich, M. Clark, B. Joo, G. Shi, R. Brower et al., *Scaling Lattice QCD beyond 100 GPUs*, [1109.2935](#).
- [12] G. P. Lepage, *The analysis of algorithms for lattice field theory*, 1989.
- [13] L. Maiani, G. Martinelli, M. L. Paciello and B. Taglienti, *Scalar Densities and Baryon Mass Differences in Lattice QCD With Wilson Fermions*, *Nucl. Phys.* **B293** (1987) 420.
- [14] S. Gusken, U. Low, K. H. Mutter, R. Sommer, A. Patel and K. Schilling, *Nonsinglet Axial Vector Couplings of the Baryon Octet in Lattice QCD*, *Phys. Lett.* **B227** (1989) 266.
- [15] J. Bulava, M. Donnellan and R. Sommer, *On the computation of hadron-to-hadron transition matrix elements in lattice QCD*, *JHEP* **01** (2012) 140 [[1108.3774](#)].
- [16] G. M. de Divitiis, R. Petronzio and N. Tantalo, *On the extraction of zero momentum form factors on the lattice*, *Phys. Lett.* **B718** (2012) 589 [[1208.5914](#)].
- [17] CSSM, QCDSF/UKQCD collaboration, A. J. Chambers et al., *Feynman-Hellmann approach to the spin structure of hadrons*, *Phys. Rev.* **D90** (2014) 014510 [[1405.3019](#)].
- [18] A. J. Chambers et al., *Disconnected contributions to the spin of the nucleon*, *Phys. Rev.* **D92** (2015) 114517 [[1508.06856](#)].
- [19] M. J. Savage, P. E. Shanahan, B. C. Tiburzi, M. L. Wagman, F. Winter, S. R. Beane et al., *Proton-Proton Fusion and Tritium β Decay from Lattice Quantum Chromodynamics*, *Phys. Rev. Lett.* **119** (2017) 062002 [[1610.04545](#)].
- [20] T. Bhattacharya, V. Cirigliano, S. Cohen, R. Gupta, H.-W. Lin and B. Yoon, *Axial, Scalar and Tensor Charges of the Nucleon from 2+1+1-flavor Lattice QCD*, *Phys. Rev.* **D94** (2016) 054508 [[1606.07049](#)].
- [21] FERMILAB LATTICE, MILC, TUMQCD collaboration, A. Bazavov et al., *Up-, down-, strange-, charm-, and bottom-quark masses from four-flavor lattice QCD*, *Phys. Rev.* **D98** (2018) 054517 [[1802.04248](#)].
- [22] E. Berkowitz, C. Bouchard, D. B. Brantley, C. Chang, M. Clark, N. Garron et al., *An accurate calculation of the nucleon axial charge with lattice QCD*, [1704.01114](#).
- [23] PNDME collaboration, T. Bhattacharya, V. Cirigliano, S. Cohen, R. Gupta, A. Joseph, H.-W. Lin et al., *Iso-vector and Iso-scalar Tensor Charges of the Nucleon from Lattice QCD*, *Phys. Rev.* **D92** (2015) 094511 [[1506.06411](#)].
- [24] R. Narayanan and H. Neuberger, *Infinite N phase transitions in continuum Wilson loop operators*, *JHEP* **03** (2006) 064 [[hep-th/0601210](#)].
- [25] M. Lüscher and P. Weisz, *Perturbative analysis of the gradient flow in non-abelian gauge theories*, *JHEP* **1102** (2011) 051 [[1101.0963](#)].
- [26] M. Lüscher, *Chiral symmetry and the Yang–Mills gradient flow*, *JHEP* **1304** (2013) 123 [[1302.5246](#)].
- [27] R. C. Brower, H. Neff and K. Orginos, *The möbius domain wall fermion algorithm*, [1206.5214](#).

- [28] E. Berkowitz, C. Bouchard, C. Chang, M. Clark, B. Joo, T. Kurth et al., *Möbius Domain-Wall fermions on gradient-flowed dynamical HISQ ensembles*, *Phys. Rev.* **D96** (2017) 054513 [1701.07559].
- [29] E. E. Jenkins and A. V. Manohar, *Baryon chiral perturbation theory using a heavy fermion Lagrangian*, *Phys. Lett.* **B255** (1991) 558.
- [30] M. Luscher, *Volume Dependence of the Energy Spectrum in Massive Quantum Field Theories. 1. Stable Particle States*, *Commun. Math. Phys.* **104** (1986) 177.
- [31] S. R. Beane and M. J. Savage, *Baryon axial charge in a finite volume*, *Phys. Rev.* **D70** (2004) 074029 [hep-ph/0404131].
- [32] S. Borsanyi et al., *High-precision scale setting in lattice QCD*, *JHEP* **09** (2012) 010 [1203.4469].
- [33] K. Symanzik, *Continuum Limit and Improved Action in Lattice Theories. 1. Principles and ϕ^{**4} Theory*, *Nucl. Phys.* **B226** (1983) 187.
- [34] K. Symanzik, *Continuum Limit and Improved Action in Lattice Theories. 2. $O(N)$ Nonlinear Sigma Model in Perturbation Theory*, *Nucl. Phys.* **B226** (1983) 205.
- [35] J. Kambor and M. Mojzis, *Field redefinitions and wave function renormalization to $O(p^{**4})$ in heavy baryon chiral perturbation theory*, *JHEP* **04** (1999) 031 [hep-ph/9901235].
- [36] A. Walker-Loud et al., *Light hadron spectroscopy using domain wall valence quarks on an Asqtad sea*, *Phys. Rev.* **D79** (2009) 054502 [0806.4549].
- [37] A. Walker-Loud, *New lessons from the nucleon mass, lattice QCD and heavy baryon chiral perturbation theory*, *PoS LATTICE2008* (2008) 005 [0810.0663].
- [38] A. Walker-Loud, *Baryons in/and Lattice QCD*, *PoS CD12* (2013) 017 [1304.6341].
- [39] T. R. Hemmert, M. Procura and W. Weise, *Quark mass dependence of the nucleon axial vector coupling constant*, *Phys. Rev.* **D68** (2003) 075009 [hep-lat/0303002].
- [40] A. Calle Cordon and J. L. Goity, *Baryon Masses and Axial Couplings in the Combined $1/N_c$ and Chiral Expansions*, *Phys. Rev.* **D87** (2013) 016019 [1210.2364].
- [41] V. Bernard and U.-G. Meißner, *The Nucleon axial-vector coupling beyond one loop*, *Phys. Lett.* **B639** (2006) 278 [hep-lat/0605010].
- [42] T. Becher and H. Leutwyler, *Baryon chiral perturbation theory in manifestly Lorentz invariant form*, *Eur. Phys. J.* **C9** (1999) 643 [hep-ph/9901384].
- [43] S. Alioli, V. Cirigliano, W. Dekens, J. de Vries and E. Mereghetti, *Right-handed charged currents in the era of the Large Hadron Collider*, *JHEP* **05** (2017) 086 [1703.04751].
- [44] L. Hayen and N. Severijns, *Radiative corrections to Gamow-Teller decays*, 1906.09870.
- [45] C.-Y. Seng, M. Gorchtein, H. H. Patel and M. J. Ramsey-Musolf, *Reduced Hadronic Uncertainty in the Determination of V_{ud}* , *Phys. Rev. Lett.* **121** (2018) 241804 [1807.10197].
- [46] C. Y. Seng, M. Gorchtein and M. J. Ramsey-Musolf, *Dispersive evaluation of the inner radiative correction in neutron and nuclear β decay*, *Phys. Rev.* **D100** (2019) 013001 [1812.03352].
- [47] C.-Y. Seng and U.-G. Meißner, *Toward a First-Principles Calculation of Electroweak Box Diagrams*, *Phys. Rev. Lett.* **122** (2019) 211802 [1903.07969].
- [48] E. Berkowitz, M. A. Clark, A. Gambhir, K. McElvain, A. Nicholson, E. Rinaldi et al., *Simulating the weak death of the neutron in a femtoscale universe with near-Exascale computing*, 1810.01609.